Cancer Chemother Pharmacol (2002) 49: 7–19
DOI 10.1007/s00280-001-0380-8

ORIGINAL ARTICLE

**Merrill J. Egorin · Theodore F. Lagattuta
Deborah R. Hamburger · Joseph M. Covey
Kevin D. White · Steven M. Musser · Julie L. Eiseman**

Pharmacokinetics, tissue distribution, and metabolism of 17-(dimethylaminoethylamino)-17-demethoxygeldanamycin (NSC 707545) in CD_2F_1 mice and Fischer 344 rats

Received: 5 June 2001 / Accepted: 19 September 2001 / Published online: 30 October 2001

Abstract *Purpose*: 17-(Dimethylaminoethylamino)-17-demethoxygeldanamycin (17DMAG) is an analogue of the benzoquinone ansamycin compound 17-(allylamino)-17-demethoxygeldanamycin (17AAG), which is currently being evaluated in clinical trials. Studies were performed in mice and rats to: (1) define the plasma pharmacokinetics, tissue distribution, and urinary excretion of 17DMAG after i.v. delivery; (2) define the bioavailability of 17DMAG after i.p. and oral delivery; (3) characterize the biliary excretion of 17DMAG after i.v. delivery to rats; and (4) characterize, if possible, any metabolites of 17DMAG observed in plasma, tissue, urine, or bile. *Materials and methods*: Studies were performed in female, CD_2F_1 mice or male Fischer 344 rats. In preliminary toxicity studies and subsequent i.v. pharmacokinetic studies in mice, 17DMAG i.v. bolus doses of 33.3, 50, and 75 mg/kg were used. In bioavailability studies, i.p. and oral 17DMAG doses of 75 mg/kg were used. In preliminary toxicity studies in rats, i.v. bolus doses of 10 and 20 mg/kg were used, and in i.v. pharmacokinetic studies 10 mg/kg was used. Compartmental and noncompartmental analyses were applied to the plasma concentration versus time data. In mice and rats, concentrations of 17DMAG were determined in multiple tissues. Urine was collected from mice and rats treated with each of the i.v. doses of 17DMAG mentioned above, and drug excretion was calculated until 24 h after treatment. Biliary excretion of 17DMAG and metabolites was studied in bile duct-cannulated rats given a 10 mg/kg i.v. bolus dose of 17DMAG. 17DMAG metabolites were identified with LC/MS. *Results*: A 75 mg/kg dose of 17DMAG caused no changes in appearance, appetite, waste elimination, or survival of treated mice as compared to vehicle-treated controls. Bolus i.v. delivery of 17DMAG at 75 mg/kg produced "peak" plasma 17DMAG concentrations between 18 and 24.2 μg/ml in mice killed at 5 min after injection. Sequential reduction in the 17DMAG dose to 50 and 33.3 mg/kg resulted in "peak" plasma 17DMAG concentrations between 9.4 and 14.4, and 8.4 and 10.5 μg/ml, respectively. Plasma 17DMAG AUC increased from 362 to 674 and 1150 μg/ml·min when the 17DMAG dose increased from 33.3 to 50 and 75 mg/kg, respectively, corresponding to a decrease in 17DMAG CL_{tb} from 92 ml/min per kg to 75 and 65 ml/min per kg. Plasma 17DMAG concentration versus time data were best fit by a two-compartment open linear model. No potential 17DMAG metabolites were observed in plasma. 17DMAG bioavailability was 100% and 50% after

This work was supported by contract NO1-CM07106 and grant 2P30 CA47904 awarded by the National Cancer Institute.

M.J. Egorin (✉) · T.F. Lagattuta · D.R. Hamburger
J.L. Eiseman
Molecular Therapeutics/Drug Discovery Program,
University of Pittsburgh Cancer Institute,
Pittsburgh, PA 15213, USA
E-mail: egorinmj@msx.upmc.edu
Tel.: +1-412-6249272
Fax: +1-412-6489856

M.J. Egorin
Division of Hematology/Oncology,
Department of Medicine,
University of Pittsburgh School of Medicine,
Pittsburgh, PA 15213, USA

M.J. Egorin · J.L. Eiseman
Department of Pharmacology,
University of Pittsburgh School of Medicine,
Pittsburgh, PA 15213, USA

J.M. Covey
Toxicology and Pharmacology Branch,
Developmental Therapeutics Program,
Division of Cancer Treatment and Diagnosis,
National Cancer Institute, Bethesda,
MD 20892, USA

K.D. White · S.M. Musser
Instrumentation and Biophysics Branch,
Center for Food Safety and Applied Nutrition,
Food and Drug Administration, Washington,
DC 20204, USA

M.J. Egorin
University of Pittsburgh Cancer Institute,
E1040 Biomedical Sciences Tower,
200 Lothrop Street, Pittsburgh,
PA 15213, USA

i.p. and oral delivery, respectively. In rats, an i.v. bolus dose of 10 mg/kg produced peak plasma 17DMAG concentrations between 0.88 and 1.74 μg/ml. Plasma 17DMAG concentrations had fallen below the lower limit of quantitation by 180 min and were best fit by a one-compartment open linear model. The plasma 17DMAG AUC was 104 μg/ml·min, corresponding to a 17DMAG CLtb of 96 ml/min per kg. 17DMAG distributed rapidly to all mouse and rat tissues except brain and testes. Only mouse liver contained materials consistent with potential metabolites of 17DMAG, but their concentrations were below the limit of quantitation of the HPLC assay used. Within the first 24 h after delivery, urinary excretion of 17DMAG by mice and rats accounted for 10.6–14.8% and 12.5–16%, respectively, of the delivered dose. By 15 min after i.v. delivery of 10 mg/kg of 17DMAG, rat bile contained 11 new materials with absorbance similar to that of 17DMAG. Four of these proposed metabolites had an M_r of 633, indicating addition of an oxygen. Two of these proposed metabolites had an M_r of 603, implying the loss of one methyl group, and one had an M_r of 589, implying the loss of two methyl groups. The remaining four proposed metabolites had an M_r of 566, 571, 629, and 645, respectively. Biliary excretion of 17DMAG and metabolites accounted for $4.7 \pm 1.4\%$ of the delivered dose, with 17DMAG accounting for $50.7 \pm 3.4\%$ of the biliary excretion. *Conclusions*: 17DMAG has excellent bioavailability when given i.p. and good bioavailability when given orally. 17DMAG is widely distributed to tissues and is quantitatively metabolized much less than is 17AAG. The pharmacokinetic and metabolite data generated should prove relevant to the design of additional preclinical studies as well as to contemplated clinical trials of 17DMAG and could be useful in their interpretation.

Keywords Geldanamycin · Ansamycin · HSP90 · Pharmacokinetics

Introduction

Geldanamycin (Fig. 1), a benzoquinone ansamycin antibiotic related to herbimycin A, has potent antiproliferative activity [5, 29, 35, 39, 43, 47, 48, 58, 69]. Furthermore, this antiproliferative activity correlates with the ability of geldanamycin to deplete oncoproteins such as $p185^{erbB2}$, mutant p53, and Raf-1 [5, 16, 18, 29, 35, 37, 38, 42, 47, 48, 51, 56, 58, 59]. Although the exact mechanism by which geldanamycin depletes cells of these oncoproteins continues to be characterized, it is thought to be mainly related to the ability of geldanamycin to bind specifically to heat shock protein 90 and its homologue, GRP94, thereby destabilizing the heteroprotein complexes they form with oncoproteins [5, 6, 13, 14, 24, 25, 31, 32, 41, 46, 50, 52, 55, 57, 63, 64, 65, 66, 68, 70].

As part of an effort to develop novel, potent, and selective inhibitors of $p185^{erbB2}$ that might also be useful antitumor agents, a number of geldanamycin derivatives have been synthesized and characterized biologically to varying degrees [47, 48]. One of these derivatives, 17-(allylamino)-17-demethoxygeldanamycin (17AAG; NSC 330507) [36, 49], was selected for clinical development and has recently been introduced into phase I testing [3, 9, 10, 15, 21, 34, 67]. Despite its introduction into clinical trials, 17AAG has several potential drawbacks. It is known to undergo metabolism to potentially toxic metabolites [19] and requires formulation in a relatively complex vehicle. As a result of these issues, there has been an ongoing effort to develop additional geldanamycin analogues that might have advantages over

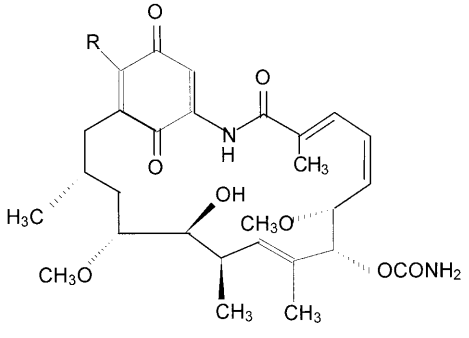

Fig. 1 Structures of geldanamycin, 17-(allylamino)-17-demethoxygeldanamycin, 17-(amino)-17-demethoxygeldanamycin, and 17-(dimethylaminoethylamino)-17-demethoxygeldanamycin

Compound	R	Molecular Weight
Geldanamycin	CH_30	560
17-(allylamino)-17-demethoxygeldanamycin	CH_2=CH-CH_2-NH	585
17-(amino)-17-demethoxygeldanamycin	NH_2	545
17-(dimethylaminoethylamino)-17-demethoxygeldanamycin	$(CH_3)_2$NH- CH-CH_2-NH	617

17AAG. One of these, 17-(dimethylaminoethylamino)-17-demethoxygeldanamycin (17DMAG; NSC 707545), is currently undergoing preclinical evaluation in preparation for clinical trials. In the NCI 60-cell panel in vitro activity screen, the GI_{50} of 17DMAG was $0.051 \pm 0.002\ \mu M$ as compared to the GI_{50} of $0.12\ \mu M$ for 17AAG. In addition, 17DMAG demonstrates in vivo activity against MDA-MB-231 breast cancer xenografts, NCI-H22 lung cancer xenografts, and LOX IMVI melanoma xenografts. As part of this preclinical evaluation, we performed pharmacokinetic studies of 17DMAG in mice and rats. Our intention was to define the plasma pharmacokinetics, tissue distribution, excretion and bioavailability of 17DMAG, and, if possible, also study its metabolism.

Materials and methods

Reagents

Triethylamine and formic acid (99.9%) were obtained from Sigma Chemical Co. (St. Louis, Mo.). 17AAG and 17-(amino)-17-demethoxygeldanamycin (17AG; NSC 255109; Fig. 1) were obtained from the Developmental Therapeutics Program, National Cancer Institute (Bethesda, Md.). Sodium phosphate (monobasic, certified A.C.S.), *o*-phosphoric acid (certified A.C.S.), ethyl acetate (certified A.C.S.) and acetonitrile (Optima Grade) were obtained from Fischer Scientific (Fair Lawn, N.J.).

Drug

17DMAG, supplied by the Developmental Therapeutics Program, National Cancer Institute as a lyophilized preparation, was stored in the dark and at 4–8°C until use. Dosing solutions were prepared by dissolving 17DMAG in the appropriate volume of sterile, 5% dextrose in water.

Mice and rats

Specific-pathogen-free adult female CD_2F_1 mice (5–6 weeks of age) were obtained from the animal program administered by the Biological Testing Branch of the National Cancer Institute. Male Fischer 344 rats (7–8 weeks of age) were purchased from Hilltop Lab Animals (Scottsdale, Pa.). Mice and rats were allowed to acclimate to the University of Pittsburgh Animal Facility for at least 1 week before studies were initiated. To minimize exogenous infection, mice and rats were maintained in microisolator cages in separate rooms and handled in accordance with the Guide for the Care and Use of Laboratory Animals (National Research Council, 1996). Ventilation and air flow in the animal facility were set to 12 changes per hour. Room temperature was regulated at 72 ± 2°F, and the rooms were kept on automatic 12-h light/dark cycles. Mice and rats received Prolab ISOPRO RMH 3000, Irradiated Lab Diet (PMI Nutrition International, Brentwood, Mo.) and water ad libitum except on the evening prior to dosing, when all food was removed and withheld until 4 h after dosing. Sentinel animals (CD-1 mice or Sprague-Dawley rats in cages with bedding 20% of which was bedding removed from the study animal cages at cage change) were maintained in the room housing the study animals and assayed at monthly intervals for specific murine pathogens by murine antibody profile testing (Charles River, Boston, Mass.). Sentinel animals remained free of specific pathogens throughout the study period, indicating that the study animals were free of specific pathogens.

Protein binding studies

In order to assess protein binding of 17DMAG, 10 μg/ml solutions of 17DMAG were prepared in mouse and rat plasma, and aliquots were placed into Amicon Centrifree ultrafiltration devices (Amicon Company, Danvers, Mass.). After centrifugation of the ultrafiltration devices for 20 min at 2000 *g* and room temperature, the concentrations of 17DMAG in the resulting protein-free ultrafiltrates and in the initial plasma solutions were determined with the HPLC method described below.

Range-finding studies

Groups of five female and five male CD_2F_1 mice were dosed i.v. with 33.3, 50 or 75 mg/kg 17DMAG or vehicle. Groups of five male Fischer 344 rats were dosed i.v. with 10 or 20 mg/kg 17DMAG or vehicle. Mice and rats were observed for 14 days after dosing. Clinical observations were made twice daily. Body weights were measured twice weekly. All group data, including necropsy tissue weights, were compared by both parametric and non-parametric methods using Minitab (Minitab, State College, Pa.). If one-way analysis of variance was significant, pair-wise comparisons were made using Dunnett's *t*-test. Non-parametric analyses used Kruskal-Wallace testing, followed by pair-wise comparisons by the Mann-Whitney test.

Pharmacokinetic studies

Dosing

Drug solutions were adjusted with vehicle such that each mouse at doses of 50 and 33.3 mg/kg received 0.01 ml/g fasted body weight. Mice dosed with 75 mg/kg received 0.015 ml/g fasted body weight. 17DMAG was administered as boluses to mice i.v. through a 27-gauge needle placed into a lateral tail vein, i.p. through a 27-gauge needle placed into the right lower abdominal quadrant, and orally through a 1.5-inch 20-gauge curved gavage needle. The 10 mg/kg i.v. dose of 17DMAG was delivered to rats as a bolus through a 26-gauge needle placed into a lateral tail vein in a volume of 0.005 ml/g body weight. The accuracy of each dosing solution was confirmed with the HPLC system described below.

Sampling

In all mouse studies, three mice were sampled at each time indicated. In the 75 mg/kg i.v. study, blood was sampled at 5, 10, 15, 30, 45, 60, 90, 120, 180, 240, 360, 420, 960, 1440, and 2880 min after dosing. In the 50 and 33.3 mg/kg i.v. studies, blood sampling was limited to the first 360 min after dosing. In studies in which 17DMAG was delivered either i.p. or orally, the 960- and 1440-min samples were omitted. In the study in which 17DMAG was administered i.v. at 75 mg/kg, brain, heart, lungs, liver, kidneys, spleen, fat, red blood cells and skeletal muscle were collected from each mouse at the same times noted for blood samples. In each study, blood and, if relevant, tissues from mice killed 5 min after delivery of vehicle served as controls.

In rat pharmacokinetic studies, groups of three rats were sampled at staggered times so that blood was obtained before drug delivery and at the following times after drug administration: 5, 10, 15, 30, 45, 60, 90, 120, 180, 240, 360, 420, 960, and 1440 min. Groups of rats were killed at 240, 360, 420, 960, and 1440 min after drug delivery, and brain, heart, lungs, liver, kidneys, spleen, fat, red blood cells, testes and skeletal muscle were collected from each rat. Plasma and tissues from rats injected only with vehicle served as controls.

Blood was collected from mice by cardiac puncture into heparinized syringes, transferred to Eppendorf microcentrifuge tubes and stored on ice until centrifugation at 13,000 *g* for 4 min to obtain plasma. Red blood cells were stored at –70°C. Tissues were rapidly dissected, placed on ice until weighing, and then snap-frozen

in liquid nitrogen. Sets of mice to be sampled at 960 or 1440 min after dosing were gang-housed in metabolism cages, and urine was collected on ice until the animals were killed for blood and, if necessary, tissue sampling. The first two blood samples from each rat were obtained through indwelling jugular venous catheters. At the time of the third blood sample, rats were exsanguinated by cardiac puncture. Plasma was prepared from rat blood and rat tissues were dissected and handled as described above for mouse samples.

Biliary excretion of 17DMAG was studied in three rats with surgically implanted bile duct cannulae. This was accomplished by anesthetizing each animal with 40 mg/kg i.p. pentobarbital (Nembutal, Abbott Laboratories, North Chicago, Ill.), isolating its bile duct through a midline abdominal incision, and cannulating the bile duct with a 28-gauge L-Cath Peel Away polyurethane catheter (Luther Medical Products, Tustin, Calif.). After the cannula had been secured proximally and distally with 2-0 silk sutures and allowed to drain under gravity, the abdominal wound was closed with Michel wound clips. 17DMAG was administered as a bolus dose of 10 mg/kg through a tail vein, and during the subsequent 4 h bile was collected as 15-min timed fractions in preweighed cryogenic vials (Corning, Corning, N.Y.). Anesthesia was maintained with additional 10 mg/kg i.p. doses of pentobarbital as needed, and at the conclusion of the 4-h bile collection, rats were killed with 100 mg/kg i.v. pentobarbital.

Plasma, tissues, urine, bile and dosing solutions were stored at –70°C until analysis.

Analysis of in vivo samples

Concentrations of 17DMAG in plasma, tissue, urine and bile were determined with HPLC using a modification of a previously published method [15, 16]. In anticipation of 17AG being a potential metabolite of 17DMAG, standard curves were prepared for both 17DMAG and 17AG. Plasma, bile, and red blood cells were extracted directly. Tissue samples were thawed and immediately homogenized using a Powergen 35 homogenizer (Fischer Scientific) in two to four parts (weight to volume) of phosphate-buffered saline (1.2 m*M* KH_2PO_4, 2.9 m*M* Na_2HPO_4, 154 m*M* NaCl, pH 7.2; GIBCO BRL, Life Technologies, Rockville, Md.).

Extraction procedure

To a 200-µl sample of plasma, red blood cells, tissue homogenate, or bile, was added 5 µl of 200 µg/ml 17AAG (internal standard) in acetonitrile and mixed. Each sample was extracted with 1 ml ethyl acetate by mixing for 10 min on a Vortex Genie 2 (Model G-560, Scientific Industries, Bohemia, N.Y.) set at 4. The samples were subsequently centrifuged at 14,000 *g* for 5 min, and the resulting organic layers were removed and transferred to 12 × 75-mm glass culture tubes. Each sample was extracted with an additional 1 ml ethyl acetate, vortexed, centrifuged, and the second organic layers were combined with the first. The organic layers were evaporated to dryness under a stream of nitrogen (Medical grade, Praxair, Pittsburgh, Pa.), and the dried residues were resuspended in 200 µl of the initial mobile phase described below. These samples were transferred to microcentrifuge tubes and centrifuged at 14,000 *g* for 2 min. The resulting supernatants were placed into glass microvial inserts, and 150 µl was injected by autosampler into the HPLC system. Urine, either undiluted or diluted 1:10 or 1:100 with the mobile phase described below, was injected directly into the HPLC system.

HPLC

The HPLC system consisted of a Waters 717 autosampler and a Waters 600E system controller and solvent delivery system fitted with a Waters Novapak C18 guard column and a Waters Novapak C18 column (5 µm, id 3.9 × 150 mm) (Waters Associates, Milford, Mass.). The initial mobile phase, consisting of acetonitrile/25 m*M* sodium phosphate, pH 3.00 (35:65 v/v) with 10 m*M* triethylamine, was pumped at 1 ml/min for 7 min. At 7.01 min, the mobile phase was changed to acetonitrile/25 m*M* sodium phosphate, pH 3.00 (50:50 v/v) with 10 m*M* triethylamine, and this was pumped isocratically until 15 min. Between 15 and 19 min, the mobile phase was returned to the initial conditions which were maintained for an additional 7 min before injection of the next sample. Column eluent was monitored at 330 nm with a Spectroflow 757 absorbance detector (ABI Analytical, Kratos Division, Ramsey, N.J.). Under these conditions, the retention times of 17AG, 17DMAG, and internal standard were approximately 5.6, 9.9, and 17.7 min, respectively, and the overall run time was 26 min.

Standard curves of 17AG and 17DMAG at concentrations of 0.15, 0.25, 0.5, 1.5, 5, 15, and 50 µg/ml in plasma, 5% dextrose in water, or control tissue homogenates were prepared in duplicate. There were no endogenous materials in plasma, any tissue, urine, bile, or dosing vehicle that interfered with the determination of 17AG, 17DMAG, or internal standard. Recovery of 17DMAG from spiked samples containing 10 µg/ml was 94 ± 1.7%. The lower limit of quantitation [53] was 0.15 µg/ml, and the coefficients of variation in plasma at a low mid-range concentration (0.5 µg/ml) and a high mid-range concentration (5 µg/ml) were 9% and 3%, respectively. The standard curves of 17AG and 17DMAG in plasma were linear between 0.15 and 50 µg/ml. Samples containing concentrations above the upper limits of each standard curve were reassayed after dilution in the appropriate matrix to a degree calculated to produce concentrations within the linear range. Plasma quality control samples, prepared at 0.25, 2.5, and 25 µg/ml and stored at –70°C, were included with each HPLC run. Tissue concentrations of 17DMAG were expressed as micrograms per gram, based on the assumption that the weight of 1 ml of homogenate was 1 g. Biliary metabolites for which authentic standards were not available were expressed as 17DMAG equivalents.

Pharmacokinetic analysis

The time courses of plasma concentrations of 17DMAG were analyzed by both noncompartmental and compartmental methods. The area under the curve from zero to infinity (AUC) and the terminal half-life (t1/2) were estimated by noncompartmental analysis using the LaGrange function [71], as implemented by the computer program LAGRAN [40]. Total body clearance (CLtb) was calculated from the equation:

$$\mathrm{CLtb} = \mathrm{Dose}/\mathrm{AUC},$$

The steady-state volume of distribution (Vdss) was calculated from the equation:

$$\mathrm{Vdss} = \mathrm{Dose} \times \left(\mathrm{AUMC}/\mathrm{AUC}^2\right),$$

where AUMC is the area under the moment curve from 0 to infinity. Tissue AUCs were also calculated using the LaGrange function.

Individual concentrations of 17DMAG detected in plasma versus time were fit to compartmental models with the program ADAPT II [17], using maximum likelihood estimation. Two- and three-compartment open linear models were fit to the data. Model discrimination was based on Akaike's information criterion (AIC) [4], calculated as:

$$\mathrm{AIC} = 2p + n(\ln \mathrm{WSSR})$$

where p represents the number of parameters, n is the number of observations and WSSR is the weighted sum of squares residuals.

Metabolite characterization and identification

Absorbance spectra of 17DMAG and proposed metabolites in tissue, urine, and bile were obtained using the same columns and mobile phase described above. Column eluate was monitored for absorbance between 200 and 600 nm with a Hewlett-Packard 1050

diode array detector and a Hewlett-Packard Chemstation operating under Microsoft Windows 95-based software.

LC/MS analyses used a Hewlett-Packard model 1050 pump that provided linear gradients and a constant flow rate of 200 µl/min. All chromatography was performed on a Waters YMC J-sphere ODS-M80 column (2 × 250 mm) packed with 4-µm particles. A 25-min gradient starting with acetonitrile/0.1% formic acid in water (5:95 v/v) and ending with acetonitrile/0.1% formic acid in water (50:50 v/v) was used for elution of 17DMAG metabolites. Mass spectrometry was performed on a Finnigan (San Jose, Calif.) model TSQ-7000 triple quadrupole mass spectrometer equipped with a standard Finnigan electrospray ion source. Materials absorbing at 330 nm were detected in-line with a Hewlett-Packard model 1100 diode array detector prior to entry into the mass spectrometer. Mass spectra were acquired in the positive ion mode at a rate of one scan per second over a mass range of 150–900 Da.

Results

Plasma protein binding

When a 10 µg/ml solution of 17DMAG in distilled water was centrifuged in a Centrifree device, 80 ± 2% of the 17DMAG passed through the ultrafiltration membrane. When 10 µg/ml solutions of 17DMAG in mouse and rat plasma were processed in a similar manner and accounting for the non-specific binding described above, 69.2 ± 4.8% (mean ± SD) and 60.4 ± 1.7% of the 17DMAG were ultrafilterable, implying that only 30–40% of 17DMAG was protein-bound.

Range-finding study

No changes were noted in appearance, appetite, waste elimination or body weight of treated mice when compared to untreated controls. None of the rats treated with DMAG died, and all gained weight after DMAG treatment. However, rats treated with 10 mg/kg gained weight at a rate comparable to vehicle-treated controls, whereas the rate of weight gain of rats treated with 20 mg/kg was significantly less than that of controls and rats treated with 10 mg/kg.

Pharmacokinetic studies

Mice

Because no untoward effects were noted in the range-finding study, the maximum dose used in i.v. pharmacokinetic studies was 75 mg/kg.

After an i.v. dose of 75 mg/kg, "peak" plasma 17DMAG concentrations at 5 min after injection were 18–24.2 µg/ml (Fig. 2). Thereafter, plasma 17DMAG concentrations declined in a manner best fit by a two-compartment open linear model (Table 1) and after 420 min were below the lower limit of quantitation. When calculated with noncompartmental methods, the 17DMAG AUC produced by a 75 mg/kg i.v. dose was 1150 µg/ml·min, corresponding to a CLtb of 65 ml/min per kg (Table 2). Sequential dose reduction to 50 and 33.3 mg/kg resulted in the expected lower plasma 17DMAG concentrations and AUCs (Fig. 2, Table 2). After i.v. doses of 50 and 33.3 mg/kg, "peak" plasma 17DMAG concentrations were between 9.4 and 14.4 and 8.4 and 10.5 µg/ml, respectively. As with the 75 mg/kg i.v. dose, the 17DMAG concentration versus time profiles resulting from the 50 and 33.3 mg/kg doses were best fit by a two-compartment open linear model (Table 1). The 17DMAG AUCs resulting from the 50 and 33.3 mg/kg i.v. doses were 675 and 362 µg/ml·min,

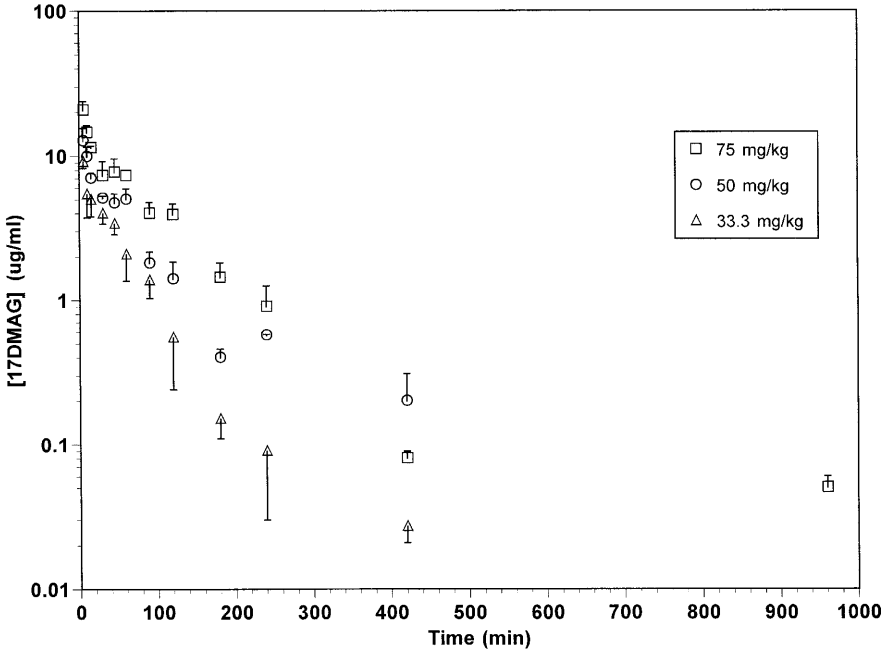

Fig. 2 Concentrations of 17DMAG detected in plasma of female CD_2F_1 mice given 17DMAG i.v. at doses of 75 mg/kg (*squares*), 50 mg/kg (*circles*), or 33.3 mg/kg (*triangles*). Symbols represent the means of three mice at each time point, and error bars represent one SD

Table 1 Pharmacokinetic parameters resulting from fitting of compartmental models to plasma 17DMAG concentration-versus-time data from CD_2F_1 mice (*Vc* volume of the central compartment, *ke* elimination constant, *kcp* transfer constant between central and peripheral compartments, *kpc* transfer constant between peripheral and central compartment, *ka* absorption constant, *t1/2α* alpha half-life, *t1/2β* beta half-life, *CLtb* total body clearance, *Vdss* steady-state volume of distribution; *NA* not applicable)

Dose (mg/kg)	Route	Vc (ml/kg)	ke (min^{-1})	kcp (min^{-1})	kpc (min^{-1})	ka (min^{-1})	t1/2α (min)	t1/2β (min)	CLtb ($ml \cdot min^{-1} \cdot kg$)	Vdss (ml/kg)
75	i.v.	437	0.119	0.418	0.058	NA	1.2	59	52	3159
50	i.v.	830	0.080	0.321	0.089	NA	1.4	46	67	3006
33.3	i.v.	2039	0.041	0.133	0.121	NA	2.5	39	83	2039
75	i.p.	5567	0.011	NA	NA	0.136	63	NA	61[a]	NA
75	oral	1366	0.079	0.168	13.7	0.0058	0.05	9	108[a]	17

[a]Apparent clearance

Table 2 Noncompartmental pharmacokinetic analyses of 17DMAG plasma concentration-versus-time curves from CD_2F_1 mice ($AUC_{0\text{-}inf}$ area under the curve from time zero to infinity, *t1/2* terminal half-life, *Vdss* steady-state volume of distribution, *CLtb* total body clearance; *NA* not applicable)

Dose (mg/kg)	Route	$AUC_{0\text{-}inf}$ ($\mu g \cdot ml^{-1} \cdot min$)	t1/2 (min)	Vdss (ml/kg)	CLtb ($ml \cdot min^{-1} \cdot kg$)	Bioavailability (%)
75	i.v.	1150	88	5400	65	NA
50	i.v.	675	79	6700	75	NA
33.3	i.v.	362	69	5060	92	NA
75	i.p.	1170	44	6090	64[a]	100
75	oral	575	52	18200	130[a]	50

[a]Apparent clearance

respectively, corresponding to CLtb values of 75 and 92 ml/min per kg, respectively (Table 2).

In none of these studies was there any material in the plasma that was not present in the plasma of vehicle-treated control mice or in the dosing solution used in any study. Specifically, there was no evidence of 17AG or any other metabolite of 17DMAG.

During the 24 h after i.v. doses of 75, 50, or 33.3 mg/kg, between 10.6% and 14.8% of the delivered dose could be accounted for in the urine. This was essentially all in the form of 17DMAG. Urine did show two small peaks with retention times of approximately 4 and 5 min, respectively, that had absorbance spectra similar to that of 17DMAG (Fig. 3A, B).

Analyses of tissue concentrations of 17DMAG allowed description of the widespread distribution of the drug, the relative inability of 17DMAG to cross the blood-brain barrier, and the relative exposures of tissues as opposed to plasma. After i.v. delivery of the 75 mg/kg dose, 17DMAG was widely distributed to tissues (Table 3). The highest tissue concentrations of 17DMAG were found in liver and kidneys, with progressively lower concentrations being found in heart, lung, spleen, red blood cells, skeletal muscle, fat, and brain. Although 17DMAG concentrations in all tissues declined with time, 17DMAG was detected in all tissues for at least 6 h after drug delivery and persisted in spleen and liver for 24 h (Table 3). When expressed as AUC, the exposure of most tissues to 17DMAG was substantially greater than that of plasma (Table 3). Only liver contained evidence of putative 17DMAG metabolites (Fig. 4A, B), but the concentrations of these materials were too low to quantify.

After completion of the three i.v. pharmacokinetic studies described above, an effort was made to define the bioavailability of 17DMAG after i.p. and oral delivery. After i.p. delivery of the 75 mg/kg dose of 17DMAG, plasma concentrations of 17DMAG increased rapidly, with peak concentrations of approximately 10 μg/ml between 10 and 45 min, and then declined to less than the lower limit of quantitation by 420 min (Fig. 5). Modeled in a noncompartmental fashion, the 17DMAG AUC produced by the 75 mg/kg i.p. dose was 1170 μg/ml·min, indicating a bioavailability of 100% (Table 2). In addition to modeling these plasma concentration versus time data in a noncompartmental fashion, compartmental modeling was also employed. The data were best fit by a one-compartment open linear model with first-order absorption from the peritoneum, and resulted in values for V, ka, and ke of 5567 ml/kg, 0.1361 min^{-1}, and 0.011 min^{-1}, respectively (Table 1).

A final mouse pharmacokinetic study was undertaken wherein a 75 mg/kg dose of 17DMAG was administered by gavage (Fig. 5). Peak plasma 17DMAG concentrations of approximately 3 μg/ml were found at between 10 and 60 min after administration of drug. Modeled in a noncompartmental fashion, the 17DMAG AUC produced by the 75 mg/kg oral dose was 575 μg/ml·min, indicating a bioavailability of 50% (Table 2). In addition to modeling these plasma concentration versus time data in a noncompartmental fashion, compartmental modeling was also employed. The data were best fit by a two-compartment open linear model with first-order absorption, and resulted in values for V, ka, kcp, kpc, and ke of 1366 ml/kg, 0.058 min^{-1}, 0.168 min^{-1}, 13.7 min^{-1}, and 0.079 min^{-1}, respectively (Table 1).

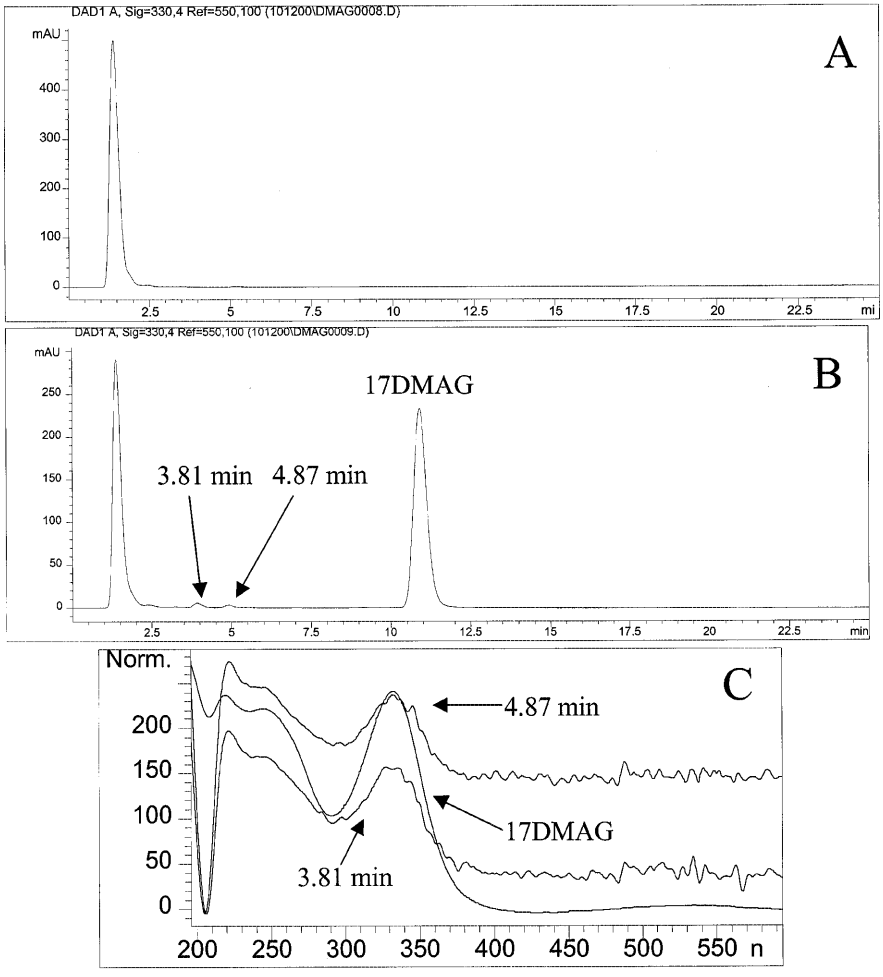

Fig. 3A–C **A, B** HPLC chromatograms of pooled urine voided between 0 and 8 h from three mice treated i.v. with (**A**) vehicle only (control) or (**B**) 75 mg/kg DMAG. **C** Absorbance spectra of suspected 17DMAG metabolites

Table 3 Concentrations and AUCs of 17DMAG in plasma and tissues of CD_2F_1 mice injected i.v. with a 75 mg/kg dose of 17DMAG (each value is the mean of three samples)

Time (min)	Plasma (μg/ml)	Brain (μg/g)	Heart (μg/g)	Lung (μg/g)	Liver (μg/g)	Kidney (μg/g)	Spleen (μg/g)	Skeletal muscle (μg/g)	Fat (μg/g)	RBCs (μg/ml)
5	20.6	2.7	65.96	63.4	135.3	132.2	49.1	29.6	8.9	36.6
10	14.5	1.6	47.4	66.7	114.0	122.0	70.9	31.8	10.9	35.0
15	11.4	2.1	42.6	69.4	98.4	100.5	77.3	36.9	12.3	32.2
30	7.3	1.2	17.9	61.9	72.2	68.9	65.7	18.5	10.5	22.9
45	7.7	1.7	18.9	40.5	73.9	67.9	67.3	17.8	10.7	23.5
60	7.3	1.9	15.1	32.5	61.7	54.8	52.2	14.4	5.3	21.4
90	4.0	1.8	12.8	25.5	57.9	41.9	46.5	8.6	5.1	18.2
120	3.9	1.6	8.6	16.4	39.1	32.0	29.3	6.0	3.8	13.6
180	1.43	1.1	3.8	8.9	21.7	18.2	21.0	2.1	1.7	7.0
240	0.9	0.92	2.2	5.7	15.4	8.7	11.6	0.81	0.75	3.2
360	0.08	0.49	0.52	2.5	5.1	2.1	6.6	0.36	0.40	0.44
420	0.05	0.64	0.24	2.0	5.2	1.7	5.0	0.05	0.11	0.27
960	0	0.37	0	0.04	0.7	0.1	0.5	0	0	0
1440	0	0.11	0	0	0.4	0	0.15	0	0	0
AUC[a]	1073	872	2939	6502	13924	10213	11351	2186	1157	3627

[a]Units: μg/ml·min for plasma or μg/g·min for tissues

Rats

After an i.v. dose of 10 mg/kg, ''peak'' plasma 17DMAG concentrations at 5 min after injection were 0.88–1.74 μg/ml (Fig. 6). Although 17DMAG could be detected in plasma until 960 min after injection, concentrations of 17DMAG were below the lower limit of quantitation after 180 min. The decline in plasma

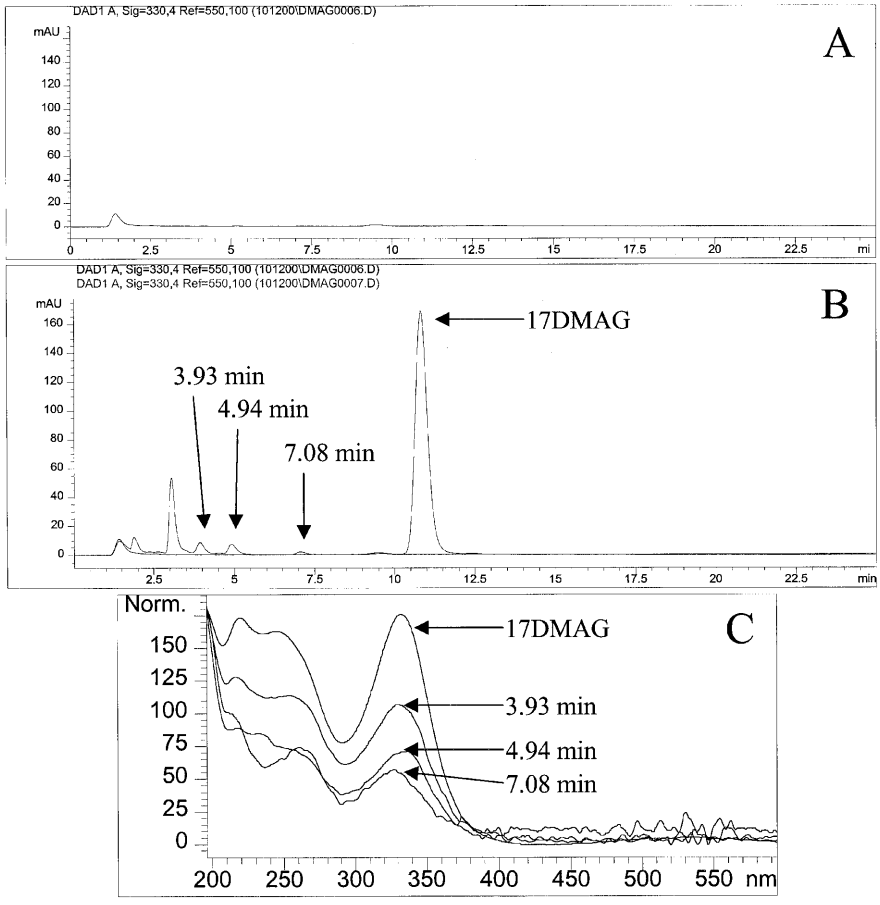

Fig. 4A–C **A, B** HPLC chromatograms of a liver extract from a mouse treated i.v. with (**A**) vehicle only (control) or (**B**) 75 mg/kg DMAG. **C** Absorbance spectra of suspected 17DMAG metabolites

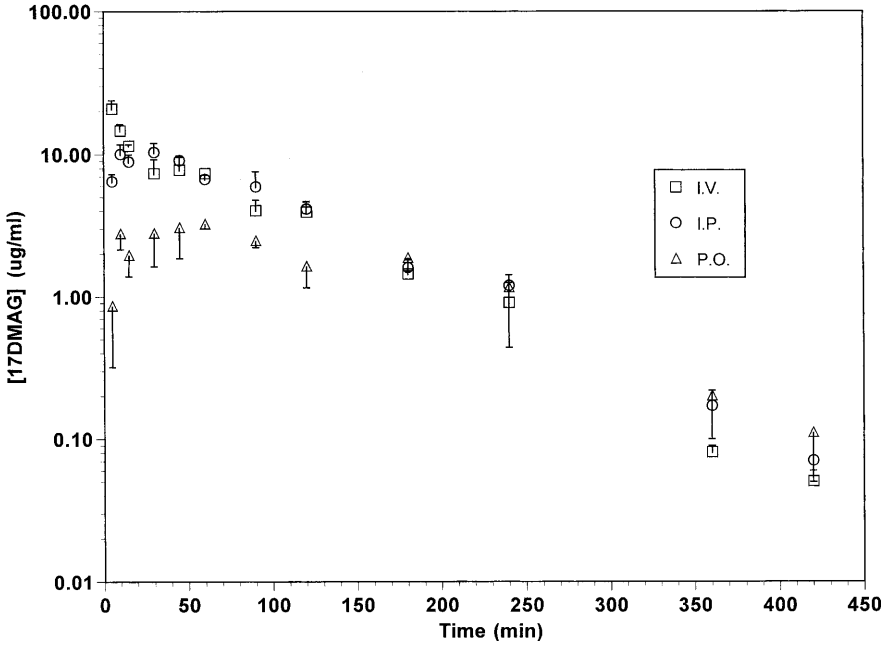

Fig. 5 Concentrations of 17DMAG detected in plasma of female CD_2F_1 mice given 75 mg/kg doses of 17DMAG i.v. (*squares*), i.p. (*circles*) or orally (*triangles*). Symbols represent the means of three mice at each time-point, and error bars represent one SD

17DMAG concentrations was best fit by a one-compartment open linear model with values for Vc, ke, t1/2, and CLtb of 6187 ml/kg, 0.015 min^{-1}, 46 min, and 94 ml/min per kg, respectively. When calculated with noncompartmental methods, the 17DMAG AUC produced by a 10 mg/kg i.v. dose was 104 μg/ml·min,

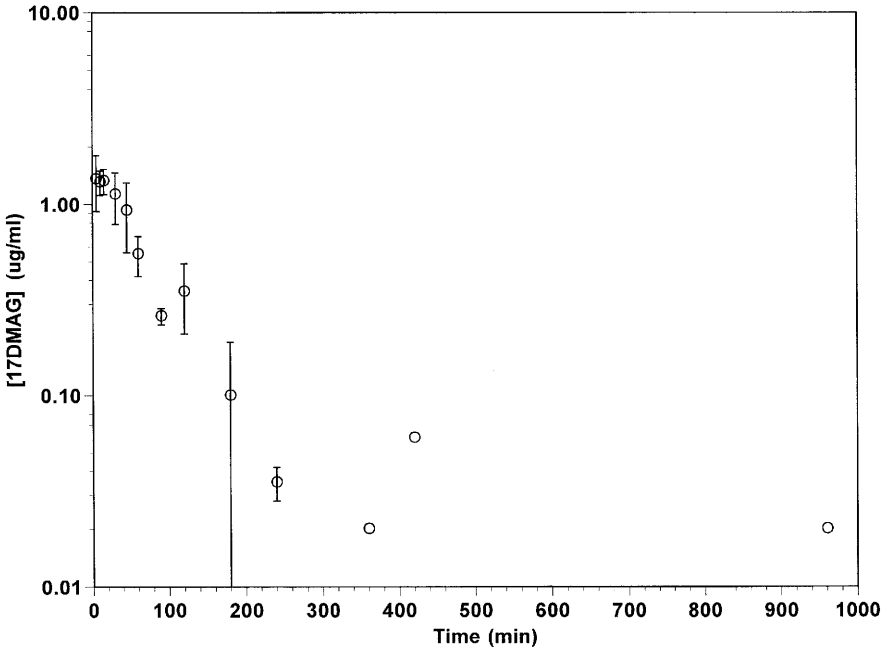

Fig. 6 Concentrations of 17DMAG detected in plasma of male Fischer 344 rats given a 10 mg/kg i.v. dose of 17DMAG. Symbols represent the means of three samples at each time-point, and error bars represent one SD

Table 4 Concentrations of 17DMAG in plasma and tissues of rats injected i.v. with a 10 mg/kg dose of 17DMAG (each value is the mean of three samples, except four plasma and RBC samples and one tissue sample at 90 min, and two plasma, RBC and tissue samples at 360 min)

Time (min)	Plasma (μg/ml)	RBCs (μg/ml)	Brain (μg/g)	Heart (μg/g)	Lung (μg/g)	Liver (μg/g)	Kidney (μg/g)	Spleen (μg/g)	Skeletal muscle (μg/g)	Fat (μg/g)	Testes (μg/g)
5	1.36	0.12									
10	1.31	0.21									
15	1.33	0.12									
30	1.13	0.20									
45	0.93	0.19									
60	0.55	0.16									
90	0.26	0.09	0	4.1	6.9	22.3	12.9	15.4	2.2	1.2	0.8
120	0.35	0.13									
180	0.10	0.07									
240	0.04	0.16	0	0.9	4.9	13.0	1.7	11.0	1	0.4	0.8
360	0.02	0.05	0	0.7	3.2	8.3	1.7	10.0	0.3	0	0.7
420	0.06	0.04	0	0.6	2.9	6.7	1.2	11.7	0.6	0.3	0.7
960	0.02	0.08	0	0.2	2.4	3.7	1.0	7.6	0	0	0.7
1440	0.0	0.0	0	0.0	1.2	1.4	0.1	2.1	0	0	1.1

corresponding to a CLtb of 96 ml/min per kg. At no time did plasma contain any evidence of a 17DMAG metabolite.

Due to the structure of the sampling schedule employed, the distribution of 17DMAG to rat tissues (Table 4) could not be defined as thoroughly as the distribution to mouse tissues (Table 3). The necessity to kill one of the scheduled 360-min rats at 90 min produced the only data on the tissue concentrations of 17DMAG at any time earlier than 240 min after drug delivery. By 90 min, concentrations of 17DMAG in most tissues were greater than those in plasma (Table 4). At 90 min, the highest concentrations of 17DMAG were observed in liver, kidney, and spleen. Tissue concentrations of 17DMAG decreased with time, but even at 24 h, remained >1 μg/g in lung, liver, and spleen (Table 4). 17DMAG was not detected in brain. Due to the relatively incomplete description of the time course of 17DMAG in tissues, tissue AUCs of 17DMAG were not calculated. Using absorbance detection, there was no evidence of 17DMAG metabolites in any rat tissue.

During the first 24 h after drug delivery, urinary excretion of 17DMAG accounted for 12.5–16% of the dose administered to rats, which agreed closely with the value previously described for urinary excretion of 17DMAG by mice. There were no metabolites of 17DMAG observed in rat urine. Biliary excretion of 17DMAG accounted for $4.7 \pm 1.7\%$ of the delivered dose. In addition to 17DMAG, bile from treated rats contained 11 materials with absorbance similar to that of 17DMAG. LC/MS analyses of rat bile indicated that four of these proposed metabolites had an M_r of 633,

two had an M_r of 603, and one each had an M_r of 566, 571, 589, 629, and 645 (Fig. 7). Biliary excretion of 17DMAG and metabolites (expressed as 17DMAG equivalents) accounted for $4.7 \pm 1.4\%$ of the delivered dose, with 17DMAG accounting for $50.7 \pm 3.4\%$ of the biliary excretion. The four materials with M_r of 633 and the two with M_r of 603 were also detected in mouse urine.

Discussion

Ideally, the rational use of any drug should reflect a consideration of the pharmacology of that drug. This philosophy may receive even more emphasis in antineoplastic chemotherapy as increased effort is being devoted to developing target-directed agents [1, 2, 7, 8, 12, 22, 28, 33, 44, 45, 54]. In the specific case of 17AAG, a heat-shock protein-interactive drug that has recently entered clinical trials [3, 9, 10, 15, 21, 34, 67], a number of aspects of its pharmacology have been described [5, 6, 11, 13, 14, 16, 18, 19, 20, 24, 25, 27, 29, 30, 31, 32, 35, 36, 37, 38, 39, 41, 42, 43, 46, 47, 48, 49, 50, 51, 52, 55, 56, 57, 58, 60, 65, 66, 68, 70]. While 17AAG is undergoing clinical evaluation, there is an ongoing effort to develop other heat-shock protein-interactive agents that might not have the theoretical drawback of metabolism to potentially toxic metabolites and the practical problem of complex formulation. The data presented here represent another part of that effort. In that regard, a number of aspects of the current studies warrant discussion.

The HPLC method used to quantify 17DMAG should be applicable to clinical trials. Such measurements should facilitate integration of the pharmacokinetics of 17DMAG with the clinical effects it produces. Obviously, the HPLC method should also be applicable to additional preclinical studies that might be undertaken in concert with, or subsequent to, the initiation of clinical trials of 17DMAG.

The use of several doses and routes of delivery of 17DMAG in the studies presented allowed several other relevant aspects of 17DMAG pharmacology to be explored. Increasing doses of 17DMAG produced increased plasma concentrations and exposures of 17DMAG. In mice, the increase in 17DMAG dose from 33.3 to 50 and 75 mg/kg was associated with a small, but consistent, disproportionate increase in plasma AUC and reduction in CLtb. Whether this truly reflects saturation of a 17DMAG clearance mechanism is not known. The CLtb value of 96 ml/min per kg calculated for rats given a 10 mg/kg i.v. dose of 17DMAG agrees very well with the value of 92 ml/min per kg calculated for mice given 33.3 mg/kg.

The tissue distribution data presented demonstrate the degree of, and relative differences in, exposure to 17DMAG as well as the durations of time that 17DMAG persists in various tissues. These data are

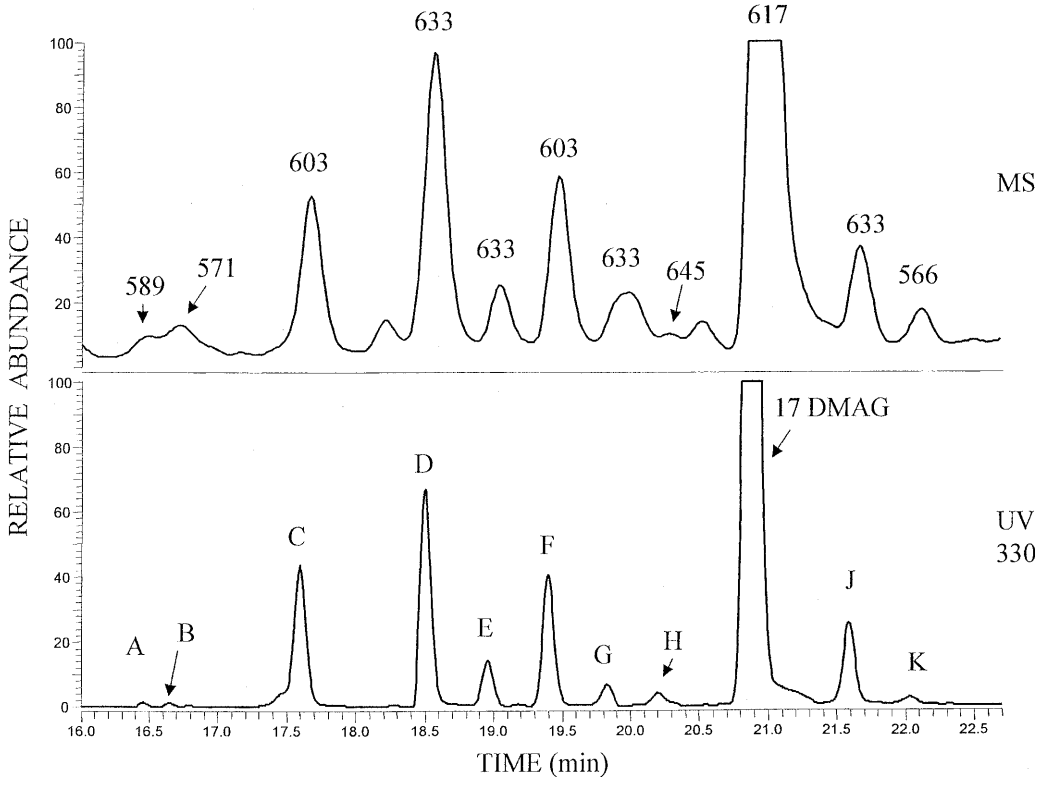

Fig. 7 Total ion chromatogram and UV absorbance chromatogram at 330 nm for an extract of bile collected from a rat given an i.v. bolus of 17DMAG at a dose of 10 mg/kg. Masses for the observed [MH]+ for each metabolite are labeled at the top of each peak in the MS chromatogram and correspond to the absorbance chromatogram as follows: *A* = 589, *B* = 571, *C* = 603, *D* = 633, *E* = 633, *F* = 603, *G* = 633, *H* = 645, *17DMAG* = 617, and *K* = 566

currently being used to construct a physiological flow model of 17DMAG pharmacokinetics, which should be of use in estimating the pharmacokinetics of this material in humans.

The results of studies in which 17DMAG was given by i.p. and oral routes showed that the bioavailability by the former route was essentially 100%, whereas the bioavailability of orally delivered 17DMAG was twice that of orally delivered 17AAG [20]. The excellent bioavailability of 17DMAG after i.p. delivery means that antitumor efficacy studies should be able to utilize that route instead of the logistically much more difficult i.v. route. The relatively good bioavailability of 17DMAG after oral administration may not be surprising. 17AAG is a known substrate for cytochrome P450 3A4 [19] and is likely a substrate for that isoform, and possibly p-glycoprotein, in the small intestine. The fact that there is relatively little metabolism of 17DMAG argues against intestinal cytochrome P450 3A4 presenting a major barrier to the bioavailability of 17DMAG. Should the oral route prove the most desirable way to produce the prolonged 17DMAG exposure that might be required for antitumor activity, this difference in oral bioavailability may represent an important advantage of 17DMAG over 17AAG.

The difference in oral bioavailability described above is only one of a number of striking differences between 17DMAG and 17AAG, a structurally closely related compound that is currently undergoing clinical evaluation. While 17AAG is >90% protein-bound [16], 17DMAG is only 30–45% protein-bound. Even more striking is the very limited quantitative metabolism of 17DMAG observed in both mice and rats, while in both species, 17AAG is known to undergo extensive metabolism by cytochrome P450 3A4 to a number of metabolites [19, 20]. Consistent with this difference in metabolism is the fact that urinary excretion of 17DMAG accounts for 10–16% of a delivered dose, as compared to the urinary excretion of only 2% of a dose of 17AAG [20]. In addition to the quantitative differences noted in the metabolism of 17DMAG and 17AAG, there are a number of qualitative differences that are notable. Although the quantitative metabolism of 17DMAG is small, the number of potential 17DMAG metabolites observed with LC/MS is much larger than the number of metabolites so far demonstrated for 17AAG, and the sites of metabolism are likely to be different.

There was no evidence that 17DMAG underwent metabolism at the 17 position to produce 17AG, the major metabolite of 17AAG. The presence of four potential 17DMAG metabolites with M_r 633 implies that oxidation can occur at four different positions on 17DMAG. The most likely places for this oxidative metabolism to occur is at the double bonds in the ansamycin ring, a site of metabolism previously not shown for 17AAG. The presence of two potential metabolites with M_r 603 implies removal of one methyl group from two different positions on 17DMAG, and the metabolite with M_r 589 presumably represents the end result of di-demethylation. These metabolites could be produced by sequential removal of the two methyl groups on the terminal amino moiety in 17DMAG, the loss of methyl groups from the two methoxy moieties on the ansamycin ring, or a combination of these processes. Although we have not definitively identified the structures of these presumed 17DMAG metabolites, they are not likely to involve alterations to the benzoquinone moiety because their absorbance spectra are not altered when compared to that of parent compound. Future studies will be directed at complete characterization of the structures of these materials, the enzymes responsible for their production and whether similar materials can be identified in the bile of rats treated with 17AAG.

In summary, we have characterized the plasma pharmacokinetics, tissue concentrations, urinary excretion and biliary excretion associated with a variety of doses and routes of administration of 17DMAG. These data should be useful in the design of additional preclinical efficacy and toxicology studies of 17DMAG and the clinical trials of 17DMAG that are being planned. Furthermore, the HPLC method developed for these studies should be applicable in those studies.

Acknowledgements We thank Diane Mazzei and her colleagues in the University of Pittsburgh Animal Facility; without their expert assistance, these studies would not have been possible. We also thank Mr. Ezekiel Woods for excellent secretarial assistance and the UPCI Hematology/Oncology Writing Group for constructive suggestions regarding the manuscript.

References

1. Adams J, Palombella VJ, Sausville EA, Johnson J, Destree A, Lazarus DD, Maas J, Pien CS, Prakash S, Elliott PJ (1999) Proteasome inhibitors: a novel class of potent and effective antitumor agents. Cancer Res 59:2615
2. Adjei AA (2000) Signal transduction pathway targets for anticancer drug discovery. Curr Pharm Des 6:361
3. Agnew EB, Neckers LM, Hehman HE, Morrison G, Hamilton JM, Monahan BP, Grem JL, Takimoto CH (2000) Human plasma pharmacokinetics of the novel antitumor agent, 17-allylaminogeldanamycin (AAG) using a new HPLC-based analytic assay. Proc Am Assoc Cancer Res 41:701
4. Akaike H (1979) A Bayesian extension of the minimal AIC procedures of autoregressive model fitting. Biometrika 66:237
5. An WG, Schnur RC, Neckers L, Blagosklonny MV (1997) Depletion of $p185^{erbB2}$, and Raf-1 and mutant p53 proteins by geldanamycin derivatives correlates with antiproliferative activity. Cancer Chemother Pharmacol 40:60
6. An WG, Schulte TW, Neckers LM (2000) The heat shock protein 90 antagonist geldanamycin alters chaperone association with p210bcr-abl and v-src proteins before their degradation by the proteasome. Cell Growth Differ 11:355
7. Arbuck SG, Takimoto CH (1998) An overview of topoisomerase I-targeting agents. Semin Hematol 35[3 Suppl 4]:3
8. Autexier C (1999) Telomerase as a possible target for anticancer therapy. Chem Biol 6:R299
9. Banerji U, Walton MI, Orr R, Kelland L, Judson IR, Workman P (2000) Development and validation of pharmacodynamic end points in tumor and normal tissue to assess the effect of the HSP90 molecular chaperone inhibitor 17-allylamino-17-demethoxy geldanamycin (17-AAG). Proc Am Assoc Cancer Res 41:721

10. Banerji U, O'Donnell A, Scurr M, Benson C, Hanwell J, Clark S, Raynaud F, Turner A, Walton M, Workman P, Judson I (2001) Phase I trial of the heat shock protein 90 (HSP90) inhibitor 17-allylamino 17-demethoxygeldanamycin (17AAG). Pharmacokinetic (PK) profile and pharmacodynamic (PD) endpoints. Proc Am Soc Clin Oncol 20:82a
11. Blagosklonny MV, Toretsky J, Neckers L (1995) Geldanamycin selectively destabilizes and conformationally alters mutated p53. Oncogene 11:933
12. Buolamwini JK (2000) Cell cycle molecular targets in novel anticancer drug discovery. Curr Pharm Des 6:379
13. Busconi L, Guan J, Denker BM (2000) Degradation of heterotrimeric Galpha(o) subunits via the proteosome pathway is induced by the hsp90-specific compound geldanamycin. J Biol Chem 275:1565
14. Chavany C, Mimnaugh E, Miller P, Bitton R, Nguyen P, Trepel J, Whitesell L, Schnur R, Moyers JD, Neckers L (1996) $p185^{erbB2}$ binds to GRP94 in vivo. J Biol Chem 271:4974
15. Clarke PA, Hostein I, George M, Maillard K, Maloney A, Walton M, Swift I, Cunningham D, Wooster R, Workman P (2000) DNA array technology in the molecular pharmacology of colorectal cancer. Proc Am Assoc Cancer Res 41:721
16. Czar MJ, Galingniana MD, Silverstein AM, Pratt WB (1997) Geldanamycin, a heat shock protein 90-binding benzoquinone ansamycin, inhibits steroid-dependent translocation of the glucocorticoid receptor from the cytoplasm to the nucleus. Biochemistry 36:7776
17. D'Argenio DZ, Schumitzky A (1979) A program package for simulation and parameter estimation in pharmacokinetic systems. Comput Methods Programs Biomed 9:115
18. Dasgupta G, Momand J (1997) Geldanamycin prevents nuclear translocation of mutant p53. Exp Cell Res 237:29
19. Egorin MJ, Rosen DM, Wolff JH, Callery PS, Musser SM, Eiseman JL (1998) Metabolism of 17-(allylamino)-17-demethoxygeldanamycin (NSC 330507) by murine and human hepatic preparations. Cancer Res 58:2385
20. Egorin MJ, Zuhowski EG, Rosen DM, Sentz DL, Covey JM, Eiseman JL (2001) Plasma pharmacokinetics and tissue distribution of 17-(allylamino)-17-demethoxygeldanamycin (NSC 330507) in CD_2F_1 mice. Cancer Chemother Pharmacol 47:291
21. Erlichman C, Toft D, Reid J, Sloan J, Atherton P, Adjei A, Ames M, Croghan G (2001) A phase I trial of 17-allyl-aminogeldanamycin in patients with advanced cancer. Proc Am Assoc Cancer Res 42:833
22. Gibbs JB (2000) Anticancer drug targets: growth factors and growth factor signaling. J Clin Invest 105:9
23. Gomez DY, Wacher VJ, Tomlanovich SJ, Herbert MF, Benet LZ (1995) The effects of ketoconazole on the intestinal metabolism and bioavailability of cyclosporine. Clin Pharmacol Ther 58:15
24. Grenert JP, Sullivan WP, Fadden P, Haystead TA, Clark J, Mimnaugh E, Krutzch H, Ochel HJ, Schulte TW, Sausville E, Neckers LM, Toft DO (1997) The amino-terminal domain of heat shock protein 90 (hsp90) that binds geldanamycin is an ATP/ADP switch domain that regulates hsp90 conformation. J Biol Chem 272:23843
25. Hartman F, Horak EM, Cho C, Luupu R, Bolen JB, Stetler SM, Pfreundschuh M, Waldmann TA, Horak ID (1997) Effects of the tyrosine-kinase inhibitor geldanamycin on ligand-induced Her-2/neu activation, receptor expression and proliferation of Her-2-positive malignant cell lines. Int J Cancer 70:221
26. Jordan WC (1998) The effectiveness of combined saquinavir and ketoconazole treatment in reducing HIV viral load. J Natl Med Assoc 90:622
27. Kelland LR, Sharp SY, Rogers PM, Myers TG, Workman P (1999) DT-diaphorase expression and tumor cell sensitivity to 17-allylamino,17-demethoxygeldanamycin, an inhibitor of heat shock protein 90. J Natl Cancer Inst 91:1940
28. Keshet E, Ben-Sasson SA (1999) Anticancer drug targets: approaching angiogenesis. J Clin Invest 104:1497
29. McIlwrath AJ, Brunton VG, Brown R (1996) Cell-cycle arrests and p53 accumulation induced by geldanamycin in human ovarian tumour cells. Cancer Chemother Pharmacol 37:423
30. Miller P, DiOrio C, Moyer M, Schnur RC, Bruskin A, Cullen W, Moyer JD (1994) Depletion of the erbB-2 gene product p185 by benzoquinoid ansamycins. Cancer Res 54:2724
31. Miller P, Schnur RC, Barbacci E, Moyer MP, Moyer JD (1994) Binding of benzoquinoid ansamycins to p100 correlates with their ability to deplete the erbB2 gene product p185. Biochem Biophys Res Commun 201:1313
32. Mimnaugh E, Chavany C, Neckers LM (1996) Polyubiquitination and proteasomal degradation of the p185c-erbB2 receptor protein-tyrosine kinase induced by geldanamycin. J Biol Chem 271:22796
33. Monks A, Scudiero DA, Johnson GS, Paull KD, Sausville EA (1997) The NCI anti-cancer drug screen: a smart screen to identify effectors of novel targets. Anticancer Drug Des 12:533
34. Munster PN, Tong L, Schwartz L, Larson S, Kenneson K, De La Cruz A, Rosen N, Scher H (2001) Phase I trial of 17-(allylamino)-17-demethoxygeladnamycin (17AAG) in patients (Pts) with advanced solid malignancies. Proc Am Assoc Clin Oncol 20:83a
35. Neckers L, Schulte TW, Mimnaugh E (1999) Geldanamycin as a potent anti-cancer agent: its molecular target and biochemical activity. Invest New Drugs 17:361
36. Nguyen DM, Desai S, Chen A, Weiser TS, Schrump DS (2000) Modulation of metastasis phenotypes of non-small cell lung cancer cells by 17-allylamino 17-demethoxy geldanamycin. Ann Thorac Surg 70:1853
37. Nimmanapalli R, O'Bryan E, Bhalla K (2001) Geldanamycin and its analogue 17-allylamino-17-demethoxygeldanamycin lowers Bcr-Abl levels and induces apoptosis and differentiation of Bcr-Abl-positive human leukemic blasts. Cancer Res 61:1799
38. Ochel HJ, Schulte TW, Nguyen P, Trepel J, Neckers L (1999) The benzoquinone ansamycin geldanamycin stimulates proteolytic degradation of focal adhesion kinase. Mol Genet Metab 66:24
39. Price PJ, Suk WA, Skeen PC, Spahn GJ, Chirigos MA (1977) Geldanamycin inhibition of 3-methylcholanthrene-induced rat embryo cell transformation. Proc Soc Exp Biol Med 155:461
40. Rocci ML, Jusko WJ (1983) LAGRAN program for area and moments in pharmacokinetic analysis. Comp Prog Biomed 16:203
41. Roe SM, Prodromou C, O'Brien R, Ladbury JE, Piper PW, Pearl LH (1999) Structural basis for inhibition of the Hsp90 molecular chaperone by the antitumor antibiotics radicicol and geldanamycin. J Med Chem 42:260
42. Sakagami M, Morrison P, Welch WJ (1999) Benzoquinoid ansamycins (herbimycin A and geldanamycin) interfere with the maturation of growth factor receptor tyrosine kinases. Cell Stress Chaperones 4:19
43. Sasaki K, Yasuda H, Onodera K (1979) Growth inhibition of virus transformed cells in vitro and antitumor activity in vivo of geldanamycin and its derivatives. J Antibiot (Tokyo) 32:849
44. Sausville EA, Feigal E (1999) Evolving approaches to cancer drug discovery and development at the National Cancer Institute, USA. Ann Oncol 10:1287
45. Sausville EA, Zaharevitz D, Gussio R, Meijer L, Louarn-Leost M, Kun Schultz R, Lahusen T, Headlee D, Stinson S, Arbuck SG, Senderowicz AM (1999) Cyclin-dependent kinases: initial approaches to exploit a novel therapeutic target. Pharmacol Ther 82:285
46. Schneider C, Sepp-Lorinzino L, Nimmersgen E, Ouerfelli O, Danishefsky S, Rosen N, Hartl FU (1996) Pharmacologic shifting of a balance between protein refolding and degradation mediated by Hsp90. Proc Natl Acad Sci USA 93:14536
47. Schnur RC, Corman ML, Gallaschun RJ, Cooper BA, Dee MF, Doty JL, Muzzi ML, DiOrio CI, Barbacci EG, Miller PE, Pollack VA, Savage DM, Sloan DE, Pustilnik LR, Moyer JD, Moyer MP (1995) erbB-2 Oncogene inhibition by geldanamy-

cin derivatives: synthesis, mechanism of action, and structure-activity relationships. J Med Chem 38:3813
48. Schnur RC, Corman ML, Gallaschun RJ, Cooper BA, Dee MF, Doty JL, Muzzi ML, Moyer JD, DiOrio CI, Barbacci EG, Miller PE, O'Brien AT, Morin MJ, Foster BA, Pollack VA, Savage DM, Sloan DE, Pustilnik LR, Moyer MP (1995) Inhibition of the oncogene product $p185^{erbB-2}$ in vitro and in vivo by geldanamycin and dihydrogeldanamycin derivatives. J Med Chem 38:3806
49. Schulte TW, Neckers LM (1998) The benzoquinone ansamycin 17-allylamino-17-demethoxygeldanamycin binds to HSP90 and shares important biologic activities with geldanamycin. Cancer Chemother Pharmacol 42:273
50. Schulte TW, Blagosklonny MV, Ingui C, Neckers L (1995) Disruption of the Raf-1-Hsp90 molecular complex results in destabilization of Raf-1 and loss of Raf-1-Ras association. J Biol Chem 270:24585
51. Schulte TW, Blagosklonny MV, Romanova L, Mushinski JF, Monia BP, Johnston JF, Nguyen P, Trepel J, Neckers LM (1996) Destabilization of Raf-1 by geldanamycin leads to disruption of the Raf-1MEK-mitogen-activated protein kinase signaling pathway. Mol Cell Biol 16:5839
52. Schulte TW, An WG, Neckers LM (1997) Geldanamycin-induced destabilization of Raf-q involves the proteasome. Biochem Biophys Res Commun 239:655
53. Shah VP, Midha KK, Dighe S, McGilvery IJ, Skelly JP, Yacobi A, Layloff T, Viswanathan CE, Cook CE, McDowall RD, Pittman KA, Spector S (1991) Analytical methods validation: bioavailability, bioequivalence and pharmacokinetic studies. Eur J Drug Metab Pharmacokinet 16:249
54. Shapiro GI, Harper JW (1999) Anticancer drug targets: cell cycle and checkpoint control. J Clin Invest 104:1645
55. Smith DF, Whitesell L, Nair SC, Chen S, Prapapanich V, Rimerman RA (1995) Progesterone receptor structure and function altered by geldanamycin, an hsp90-binding agent. Mol Cell Biol 15:6804
56. Stancato LF, Silverstein AM, Owens-Grillo JK, Chow YH, Jove R, Pratt WB (1997) The hsp90-binding antibiotic geldanamycin decreases Raf levels and epidermal growth factor signaling without disrupting formation of signaling complexes or reducing the specific enzymatic activity of Raf kinases. J Biol Chem 272:4013
57. Stebbins CE, Russo AA, Schneider C, Rosen N, Hartl FU, Pavletich NP (1997) Crystal structure of an Hsp90-geldanamycin complex: targeting of a protein chaperone by an antitumor agent. Cell 89:239
58. Supko JG, Hickman RL, Grever M, Malspeis L (1995) Preclinical pharmacological evaluation of geldanamycin as an antitumor agent. Cancer Chemother Pharmacol 36:305
59. Tikhomirov O, Carpenter G (2000) Geldanamycin induces ErbB-2 degradation by proteolytic fragmentation. J Biol Chem 275:26625
60. Uehara Y, Hori M, Takeuchi T, Umezawa H (1986) Phenotypic change from transformed to normal induced by benzoquinoid ansamycins accompanies inactivation of p60src in rat kidney cells infected with Rous sarcoma virus. Mol Cell Biol 6:2198
61. Van Asperen J, van Tellingen O, Sparreboom A, Schinkel AH, Borst P, Nooijen WJ, Beijnen JH (1997) Enhanced oral bioavailability of paclitaxel in mice treated with the P-glycoprotein blocker SDZ PSC 833. Br J Cancer 76:1181
62. Van Asperen J, van Tellingen O, van der Valk MA, Rozenhart M, Beijnen JH (1998) Enhanced oral absorption and decreased elimination of paclitaxel in mice cotreated with cyclosporin A. Clin Cancer Res 4:2293
63. Whitesell L, Cook P (1996) Stable and specific binding of heat shock protein 90 by geldanamycin disrupts glucocorticoid receptor function in intact cells. Mol Endocrinol 10:705
64. Whitesell L, Mimnaugh EG, De Costa B, Myers CE, Neckers LM (1994) Inhibition of heat shock protein HSP90-$pp60^{v\text{-}src}$ heteroprotein complex formation by benzoquinone ansamycins: essential role for stress proteins in oncogenic transformation. Proc Natl Acad Sci USA 91:8324
65. Whitesell L, Sutphin P, An WG, Schulte T, Blagosklonny MV, Neckers L (1997) Geldanamycin-stimulated destabilization of mutated p53 is mediated by the proteasome in vivo. Oncogene 14:2809
66. Whitesell L, Sutphin PD, Pulcini EJ, Martinez JD, Cook PH (1998) The physical association of multiple molecular chaperone proteins with mutant p53 is altered by geldanamycin, an hsp90-binding agent. Mol Cell Biol 18:1517
67. Wilson RH, Takimoto CH, Adnw EB, Morrison G, Grollman F, Thomas RR, Saif MW, Hopkins J, Allegra C, Grochow L, Szabo E, Hamilton JM, Monahan BP, Neckers L, Grem JL (2001) Phase I pharmacokinetic study of 17- (allylamino)-17-demethoxygeldanamycin (AAG) in adult patients with advanced solid tumors. Proc Am Soc Clin Oncol 20:82a
68. Xu W, Mimnaugh E, Rosser MF, Nicchitta C, Marcu M, Yarden Y, Neckers L (2001) Sensitivity of mature erbB-2 to geldanamycin is conferred by its kinase domain and is mediated by the chaperone protein hsp90. J Biol Chem 276:3702
69. Yamaki H, Suzuki H, Choi EC, Tanaka N (1982) Inhibition of DNA synthesis in murine tumor cells by geldanamycin, an antibiotic of the benzoquinoid ansamycin group. J Antibiot (Tokyo) 35:886
70. Yang J, Yang JM, Iannone M, Shih WJ, Lin Y, Hait WN (2001) Disruption of the EF-2 kinase/hsp90 protein complex: a possible mechanism to inhibit glioblastoma by geldanamycin. Cancer Res 61:4010
71. Yeh KC, Kwan KC (1978) A comparison of numerical integrating algorithms by trapezoidal, LaGrange and spline approximation. J Pharmacokinet Biopharm 6:79